

# Estrogen-related receptor- $\alpha$ antagonist inhibits both estrogen receptor-positive and estrogen receptor-negative breast tumor growth in mouse xenografts

Michael J. Chisamore,<sup>1,2</sup> Hilary A. Wilkinson,<sup>1</sup> Osvaldo Flores,<sup>1</sup> and J. Don Chen<sup>2</sup>

<sup>1</sup>Department of Molecular Endocrinology, Merck Research Laboratories, West Point, Pennsylvania and <sup>2</sup>Department of Pharmacology, University of Medicine and Dentistry of New Jersey-Robert Wood Johnson Medical School, Piscataway, New Jersey

## Abstract

Estrogen-related receptors (ERR) are orphan members of the nuclear receptor superfamily most closely related to estrogen receptors (ER). Although ER $\alpha$  is a successful target for treating breast cancer, there remains an unmet medical need especially for estrogen-independent breast cancer. Although estradiol is not an ERR ligand, ER and ERR share many commonalities and overlapping signaling pathways. An endogenous ERR ligand has not been identified; however, novel synthetic ERR $\alpha$  subtype-specific antagonists have started to emerge. In particular, we recently identified a novel compound, *N*-[(2*Z*)-3-(4,5-dihydro-1,3-thiazol-2-yl)-1,3-thiazolidin-2-yl idene]-5H dibenzo[*a,d*][7]annulen-5-amine (termed compound A) that acts specifically as an ERR $\alpha$  antagonist. Here, we show that compound A inhibited cell proliferation in ER $\alpha$ -positive (MCF-7 and T47D) and ER $\alpha$ -negative (BT-20 and MDA-MD-231) breast cancer cell lines. Furthermore, we report the differential expression of 83 genes involved in ERR $\alpha$  signaling in MCF-7 and BT-20 breast cancer cell lines. We show that compound A slowed tumor growth in MCF-7 and BT-20 mouse xenograft models, and displayed antagonistic effects on the uterus. Furthermore, a subset of genes involved in ERR $\alpha$  signaling *in vitro* were evaluated and confirmed *in vivo* by studying uterine gene expression profiles from xenograft mice. These results suggest for the first time that inhibition of ERR $\alpha$  signaling

via a subtype-specific antagonist may be an effective therapeutic strategy for ER-positive and ER-negative breast cancers. [Mol Cancer Ther 2009;8(3):672–81]

## Introduction

Estrogen-related receptor (ERR)- $\alpha$  is an orphan member of the steroid/nuclear receptor superfamily. The ERR subfamily consists of three members, ERR $\alpha$ , ERR $\beta$ , and ERR $\gamma$ , which share a high degree of amino acid homology to the estrogen receptors (ER) but do not bind natural estrogens or any other endogenous ligand (1, 2). ERR $\alpha$  was found by using the DNA-binding domain of ER $\alpha$  as a hybridization probe to screen recombinant DNA libraries (1). ERR $\alpha$  mRNA is expressed in the mouse embryo developing heart, intestine, brain, spinal cord, brown fat, and bone (3). ERR $\alpha$  is ubiquitously expressed in adult tissues with higher expression in tissues in which a high level of metabolism and fatty acid  $\beta$ -oxidation occurs, including skeletal muscle, kidney, heart, liver, and adipose (1, 4, 5). The ERR $\alpha$ -knockout phenotype is viable, fertile, and does not exhibit any apparent anatomic alterations except reduced body weight and smaller peripheral fat deposits (5). ERRs and ERs share common target genes previously shown to be important for breast cancer such as p52 (6), lactoferrin (7, 8), aromatase (9), and osteopontin (10) and exhibit cross-talk. Whereas many other members of the steroid receptor superfamily are activated by ligands (including ERs), ERRs are constitutively active without the addition of a specific ligand (11).

Three ERR $\alpha$  subtype-selective inverse agonists or antagonists have been reported in addition to the ERR $\alpha$  subtype-selective antagonists we have previously described (12). XCT790 is a selective inverse agonist reported to have an IC<sub>50</sub> of 0.37  $\mu$ mol/L in a GAL4-ERR $\alpha$  cell-based transfection assay (13). Cyclohexylmethyl-(1-*p*-tolyl-1H-indol-3-ylmethyl)-amine has been cocrystallized with the human ERR $\alpha$  LBD and a novel molecular mechanism of action for inverse agonism of ERR $\alpha$  has been proposed (14). The synthetic estrogen diethylstilbestrol (DES) was shown in a fluorescence resonance energy transfer assay to be an antagonist for the ERRs at high concentrations (2).

There are strong supporting data in the literature to consider the use of an ERR $\alpha$ -specific antagonist to treat breast cancer. ERR $\alpha$  is expressed in multiple human breast cancer cell lines, breast tumors, and in breast adipose tissue (6, 15, 16). ERR $\alpha$  expression in clinical breast cancer tumors correlates with an increased risk of disease recurrence and adverse clinical outcome (16). Moreover, ERR $\alpha$  expression is associated with an unfavorable, aggressive tumor phenotype correlating with ErbB2 (HER2, Neu)

Received 11/11/08; accepted 12/9/08; published OnlineFirst 3/10/09.

Grant support: NIH R01 grant DK52888 (J.D. Chen).

The costs of publication of this article were defrayed in part by the payment of page charges. This article must therefore be hereby marked *advertisement* in accordance with 18 U.S.C. Section 1734 solely to indicate this fact.

Requests for reprints: J. Don Chen, Department of Pharmacology, University of Medicine and Dentistry of New Jersey-Robert Wood Johnson Medical School, 675 Hose Lane, Piscataway, NJ 08854. Phone: 732-235-3292; Fax: 732-235-3974; E-mail: chenjd@umdnj.edu and Hilary A. Wilkinson, Department of Molecular Endocrinology, Merck Research Laboratories, 770 Summeytown Pike, West Point, PA 19486. E-mail: hilary\_wilkinson@merck.com

Copyright © 2009 American Association for Cancer Research.

doi:10.1158/1535-7163.MCT-08-1028

overexpression (15). Furthermore, the ERR $\alpha$  ligand DES inhibits breast cancer proliferation at high concentrations (6), and in the past, has been used in the clinic to treat breast cancer (17).

The rationale for an ERR $\alpha$  antagonist to treat breast cancer plus our recent discovery of new ERR $\alpha$  subtype-specific ligands has led to an effort to study the effects of ERR $\alpha$  antagonists on breast tumor growth. Specifically, *N*-[(2*Z*)-3-(4,5-dihydro-1,3-thiazol-2-yl)-1,3-thiazolidin-2-ylidene]-5H dibenzo[*a,d*][7]annulen-5-amine (or for simplicity, "compound A" in the present study) has the strongest antagonistic effect on the constitutive interaction between ERR $\alpha$  and nuclear coactivators among the ERR $\alpha$  ligands we identified (12). Our experimental results show that compound A slows cell proliferation in ER $\alpha$ -positive (MCF-7 and T47D) and ER $\alpha$ -negative (BT-20 and MDA-MD-231) breast cancer cell lines. We describe changes in the expression of genes involved in ERR $\alpha$  signaling in MCF-7 and BT-20 breast cancer cells treated with compound A. We further show that compound A inhibits tumor growth in MCF-7 and BT-20 mouse xenograft models while showing antagonistic effects on the uterus. Lastly, a subset of genes determined to be involved in ERR $\alpha$  signaling *in vitro* were validated *in vivo* by studying the gene expression profile in the uteri from treated mice.

## Materials and Methods

### Cell Proliferation Assays

Human breast cancer cell lines MCF-7, T47D, BT-20, and MDA-MB-231 were obtained from American Type Culture Collection and maintained as described in their product information sheets. Cells were grown in estrogen-free medium for 4 days prior to each experiment and were seeded into six-well plates. MCF-7 cell lines were seeded at 10,000 cells/well, whereas BT-20 cells were seeded at 20,000 cells/well. The following day, medium containing DMSO (vehicle), 1  $\mu$ mol/L of compound A (Merck & Co.), 10 nmol/L of 17 $\beta$ -estradiol (E2; Sigma), 3 pmol/L of E2, or 1  $\mu$ mol/L of compound A/3 pmol/L of E2 were added. MCF-7 cells were counted on days 2 to 6, 8, 10, and 12. BT-20 cells were counted on days 2, 7, and 10 to 14. MCF-7/shGFP, MCF-7/shERR $\alpha$ 2, and MCF-7/shERR $\alpha$ 3 RNAi cell lines<sup>3</sup> were counted on days 3 and 6 to 10. For dose titrations, cells were seeded into 96-well plates. MCF-7 and T47D cell lines were plated at 3,000 cells/well, BT-20 cell line at 6,000 cells/well, and MDA-MB-231 at 5,000 cells/well. On days 1, 4, and 8, cells were treated with vehicle (DMSO), compound A, or DES at the indicated concentrations (100 pmol/L–100  $\mu$ mol/L) in medium with 3 pmol/L of E2. On day 9, DNA contents were measured using the CyQuant Cell Proliferation Assay Kit (Invitrogen) according to the protocols of the manufacturer.

### RNA Extraction and cDNA Synthesis

Total RNA was extracted from MCF-7 and BT-20 cells treated with vehicle (DMSO), 3 pmol/L of E2, 5  $\mu$ mol/L of compound A, or 3 pmol/L of E2/5  $\mu$ mol/L of compound A for 2, 24, or 48 h, respectively. The RNA samples were treated with DNase I (Ambion, Inc.) and cDNA was synthesized using High-Capacity cDNA Archive Kit (Applied Biosystems).

### Quantitative Real-time Reverse Transcription-PCR

Two hundred and twenty-six genes involved in ER, cancer, and ERR $\alpha$  signaling (Supplementary Fig. S1)<sup>4</sup> were assayed using TaqMan Low-Density Custom Array cards (Applied Biosystems). Four to eight copies per gene (depending on card configuration) were present on multiple arrays. Genes assayed were selected based on the published literature. Real-time reverse transcription-PCR was done with an ABI 7900 HT sequence detection system (Applied Biosystems). The expression levels of target genes were normalized to 18S rRNA and glyceraldehyde-3-phosphate dehydrogenase as endogenous quantitative controls. Relative gene expression was calculated based on the  $\Delta\Delta$ Ct method as outlined in the Applied Biosystems User Guide. Relative gene expression values down-regulated  $\geq 1.2$ -fold or up-regulated  $> 1.2$ -fold ( $P < 0.05$ ) were reported and analyzed using Ingenuity Pathway Analysis (Ingenuity Systems). Genes showing significant differential expression were retested in the 96-well 7900 HT FAST real-time reverse transcription-PCR format to confirm low-density array results.

### Pharmacokinetic Study of Compound A

Five- to 6-week-old female ovariectomized athymic nude mice (NCR; Taconic) were implanted s.c. with 0.36 mg (60-day release) E2 pellets (Innovative Research of America). Mice were divided into two groups of 15 mice treated with either 15 or 30 mg/kg of compound A, and one group of 3 mice dosed with vehicle (10% DMSO/90% sesame oil).

Three days post-E2 implantation, mice received 5 consecutive days of compound A or vehicle (day 1–5). At 6, 12, 24, 36, and 48 h post-day 5, three mice from each treatment group were euthanized and blood was collected by cardiac puncture using Capiject (K2-EDTA) blood collection tubes (Terumo). Blood was also collected from three mice dosed with vehicle at the last time point. Plasma was isolated from the samples and sent to Charles River Laboratories for compound A plasma concentration determination using API-5000 liquid chromatography-tandem mass spectrometry (Applied Biosystems) following protein precipitation. Watson Bioanalytical LIMS (Thermo Scientific, version 7.2.0.02) was used to determine pharmacokinetic parameters based on plasma concentrations over time.

### Mouse Xenograft Models

MCF-7 ( $1 \times 10^7$ ) cells/site were injected (s.c.) into the axillary mammary fat pads of 5- to 6-week-old female

<sup>3</sup> Chisamore MJ, Wilkinson HA, Flores O, Chen JD. Characterization of a novel subtype specific estrogen related receptor  $\alpha$  antagonist in MCF-7 breast cancer cells. *Endocr Relat Cancer*. Submitted 2008.

<sup>4</sup> Supplementary material for this article is available at Molecular Cancer Therapeutics Online (<http://mct.aacrjournals.org/>).

674 *ERR $\alpha$  Antagonist Suppresses Breast Cancer Growth*

ovariectomized athymic nude mice (NCr; Taconic) that were also implanted with an E2 pellet (same as described above). After 5 weeks, mice were divided into three treatment groups consisting of 10 mice/group: (a) control vehicle (10% DMSO/90% sesame oil), (b) 15 mg/kg of compound A, and (c) 5 mg/wk of ICI-182,780 (AstraZeneca). BT-20 ( $5 \times 10^6$ ) cells/site were injected (s.c.) into the axillary mammary fat pads of 5- to 6-week-old female athymic nude mice. After 8 weeks, mice were divided into two treatment groups consisting of 11 to 15 mice/group: (a) control vehicle (10% DMSO/90% sesame oil) and (b) 30 mg/kg of compound A. Both MCF-7 and BT-20 xenograft models received s.c. injections every 3 days of either vehicle or compound A. The MCF-7 xenograft ICI-

182,780 treatment group received one s.c. injection weekly of 5 mg/animal. At the termination of the experiments, the animals were euthanized, whole body weight was measured, blood was drawn to determine compound A plasma concentration and uteri were weighed. Uteri were snap-frozen in liquid nitrogen and sent to Cogenics where total RNA was extracted. RNA samples from each treatment group were pooled, cDNA was synthesized, and 46 genes known to be involved in *ERR $\alpha$*  signaling were assayed using TaqMan Low-Density Custom Array cards (Applied Biosystems). Genes with significant differential expression were re-tested in the 96-well 7900 HT FAST real-time reverse transcription-PCR format to confirm low-density array results.

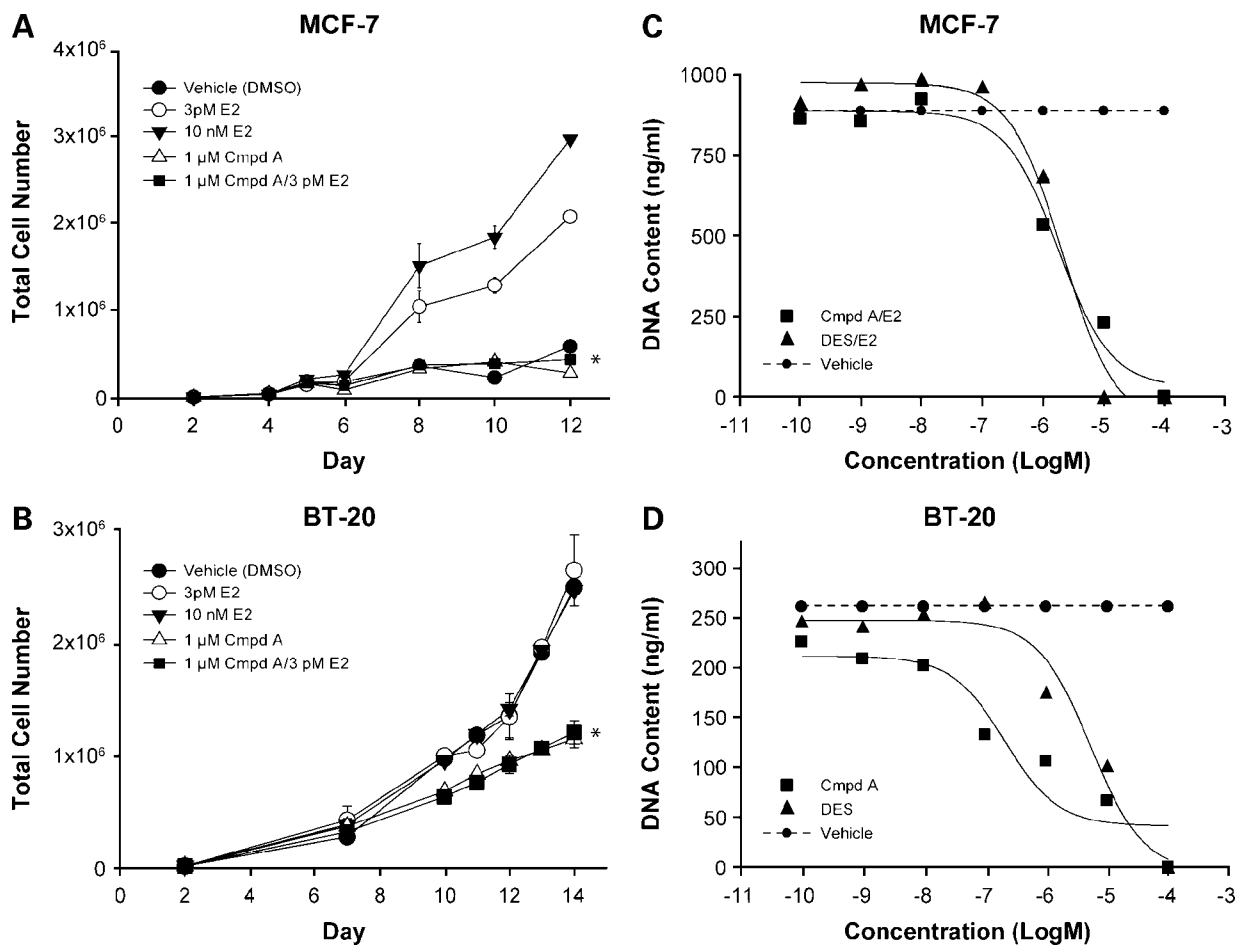


**Figure 1.** *ERR $\alpha$* -specific antagonist compound A inhibits breast cancer cell proliferation. **A**, proliferation rate of MCF-7 cells grown in E2-free medium treated with vehicle ( $\bullet$ ), 1  $\mu$ mol/L of compound A ( $\circ$ ), 10 nmol/L of E2 ( $\blacktriangledown$ ), 3 pmol/L of E2 ( $\triangle$ ), or 1  $\mu$ mol/L of compound A/3 pmol/L of E2 ( $\blacksquare$ ). **B**, proliferation rate of BT-20 cells grown in E2-free medium treated with vehicle ( $\bullet$ ), 3 pmol/L of E2 ( $\circ$ ), 10 nmol/L of E2 ( $\blacktriangledown$ ), 1  $\mu$ mol/L of compound A ( $\triangle$ ), or 1  $\mu$ mol/L of compound A/3 pmol/L of E2 ( $\blacksquare$ ). \*,  $P < 0.001$ . Differences in mean total cell number between groups [3 pmol/L E2 vs. 1  $\mu$ mol/L compound A (Cmpd A) or 1  $\mu$ mol/L compound A/3 pmol/L E2 for MCF-7 and vehicle vs. 1  $\mu$ mol/L compound A or 1  $\mu$ mol/L compound A/E2 for BT-20] were measured by ANOVA followed by a Student's  $t$  test with a 0.05 significance level. Proliferation rate was determined as outlined in Materials and Methods. Points, mean total cell number; bars, SE. **C** and **D**, growth curve of MCF-7 (**C**) and BT-20 (**D**) cells treated with vehicle ( $\bullet$ ), compound A ( $\blacksquare$ ), or DES ( $\blacktriangle$ ) at the indicated concentration (100 pmol/L – 100  $\mu$ mol/L) in medium that also contained 3 pmol/L of E2. After 9 d of treatment, DNA content was measured as outlined in Materials and Methods. The titrated dose-response curves were graphed by using GraphPad Prism, version 4.01 (GraphPad) nonlinear regression (curve fit) program.

**Table 1. IC<sub>50</sub> values of MCF7, T47D, BT-20, and MDA-MB-231 breast cancer cell lines treated with compound A or DES**

Cell line	IC <sub>50</sub> (μmol/L)	
	Compound A	DES
MCF-7 [ER (+)]	0.97	2.27
T47D [ER (+)]	1.02	1.67
BT-20 [ER (-)]	0.225	4.3
MDA-MB-231 [ER (-)]	0.65	2.2

NOTE: Compound A shows lower IC<sub>50</sub> values in the MCF-7, T47D, BT-20, and MDA-MB-231 cells in comparison to DES. GraphPad Prism, version 4.01 (GraphPad Software) was used to calculate values.

## Results

### ERR $\alpha$ -Specific Antagonist Compound A Inhibits Breast Cancer Cell Proliferation

We examined the effects of treatment with compound A on cell proliferation of the ER-positive MCF-7 and ER-negative BT-20 breast cancer cell lines. The estrogen-dependent MCF-7 cells treated with 10 nmol/L of E2 showed the most growth between days 5 and 11, followed by 3 pmol/L of E2 (Fig. 1). MCF-7 cells treated with DMSO showed little growth whereas cells treated with compound A, with or without E2, exhibited significantly reduced proliferation ( $P < 0.001$ ) versus MCF-7 cells treated with E2. Likewise, the BT-20 breast cancer cells, in which E2 does not have any effect on cell proliferation (18–20), showed significantly reduced cell proliferation ( $P < 0.001$ ) when treated with compound A compared with the vehicle group (Fig. 1B). Titrated dose-response growth curves were also carried out and reduced cell growth was shown in both MCF-7 and BT-20 cell lines (Fig. 1C and D), along with T47D and MDA-MB-231 (data not shown). After 9 days of treatment at 100 μmol/L of compound A or DES, cytotoxicity was observed. IC<sub>50</sub> for all four cell lines in response to compound A and DES were calculated (Table 1). These data show that compound A exhibits lower IC<sub>50</sub> values for all four cell lines in comparison with DES, and suggests that compound A is a more potent inhibitor of breast cancer cell proliferation.

### Differentially Expressed Genes in Breast Cancer Cells Treated with ERR $\alpha$ Antagonist

To study ERR $\alpha$  signaling in breast cancer, 226 genes known to be involved in ER, cancer, and ERR $\alpha$  signaling (Supplementary Fig. S1)<sup>4</sup> were assayed using TaqMan Low-Density Custom Array cards (Applied Biosystems). MCF-7 and BT-20 breast cancer cells were treated with vehicle (DMSO) or compound A for 2, 24, and 72 hours. Relative gene expression values (83 genes in total) that were down-regulated or up-regulated by >1.2-fold ( $P < 0.05$ ) are reported (Fig. 2).

In the MCF-7 cell line, after 2 hours of treatment with compound A, 20 genes were down-regulated, 4 were up-regulated, and 1 gene (*ELF3*) that was down-regulated when treated with compound A was also up-regulated when treated with E2. After 24 hours of treatment with

compound A, 31 genes were down-regulated whereas 6 were up-regulated. In addition, 4 genes increased whereas 9 genes decreased expression when treated with E2. Nine of the 20 genes that were down-regulated at 2 hours when treated with compound A were also down-regulated at 24 hours. After 72 hours, 30 genes decreased whereas 24 increased expression when treated with compound A. Furthermore, 12 genes were down-regulated, whereas 22 were up-regulated when treated with E2. Twenty of the 31 genes down-regulated at 24 hours were also down-regulated at 72 hours when treated with compound A. Finally, there were 7 genes that showed decreased expression at all three time points in MCF-7 cells when treated with compound A.

In the ER-negative BT-20 cells treated with compound A, 18 genes were down-regulated at 2 hours; at 24 hours, 18 genes were down-regulated whereas 3 were up-regulated. Eight of the 18 genes down-regulated at 2 hours were also decreased at the 24-hour time point. At 72 hours, 20 genes were down-regulated whereas 6 were up-regulated. In addition, 14 genes that were down-regulated and 1 gene that was up-regulated were the same genes at both the 24-hour and 72-hour time points. Finally, 7 genes were down-regulated at all three time points. Among these 7 genes, one (*HSD3B1*) was also down-regulated at all three time points in MCF-7 cells treated with compound A.

Subsequently, using gene expression data from both MCF-7 and BT-20 cell lines, Ingenuity Pathway Analysis was used to model potential ERR $\alpha$  signaling pathways affected by compound A. At 2 hours of treatment, all seven genes that were decreased in both cell lines (including two that were decreased by <1.2-fold) were built into one signaling pathway (Fig. 3A). Except for phosphorylation of ERR $\alpha$  by mitogen-activated protein kinase 3, no signaling directly involves ERR $\alpha$  (ESRRA) at this short time point. At 24 hours, 13 genes were commonly decreased in both cell lines, and 11 were modeled into a single network involving energy metabolism (Fig. 3B). These include the key enzyme ACADM involved in the mitochondrial  $\beta$ -oxidation of fat, the nuclear receptor coactivator PGC-1 $\alpha$ , and carnitine acetyltransferase which is critical for energy homeostasis and fat metabolism (21). At 72 hours of treatment, 14 out of the 19 genes affected in both cell lines also fit into a single network involving ERR $\alpha$  signaling (Fig. 3C). Similar to the 24-hour time point, ACADM, PGC-1 $\alpha$ , and SPP1 are again shown to have a direct relationship with ERR $\alpha$ . Additionally, HMGB2, a DNA-binding protein, known to bind ER $\alpha$  and ER $\beta$  (22), was up-regulated. Thus, along with energy metabolism, disrupting ERR $\alpha$  signaling in breast tumors may alter other relevant gene functions and pathways.

### Compound A Inhibits the Growth of Breast Tumors in Mouse Xenograft Models

To study the efficacy of compound A *in vivo* for treating breast cancer, we first determined the pharmacokinetic parameters of compound A in ovariectomized athymic nude mice implanted with E2 pellets and treated with compound A. Plasma concentrations of compound A were



676 *ERR $\alpha$  Antagonist Suppresses Breast Cancer Growth*

Gene	MCF-7/Cmpd A			MCF-7/E2			BT-20/Cmpd A		
	2h	24h	72h	2h	24h	72h	2h	24h	72h
ACADM		-8.55	-1.45					-5.56	-1.67
ACSS2		-1.50							
ADRB3	-1.33	-2.06	-1.59						
APC			1.25						
BCAR1			-1.80			-1.75			
BCAR3			-1.72			-1.68			
BRCA1			1.25			1.71			
BRMS1			1.36			1.48			
CD44	1.30	1.72		3.58	5.00				-2.31
CEBPB			2.12			2.06			
CEBPG			1.76			1.42			1.22
CRAT		-5.20	-3.55				-1.92	-5.63	-21.69
CREM	-1.28								
CTBP1			1.49				-1.85		
CYP1B1			1.32			1.88			
CYP19A1	-2.04	-1.64						-4.74	-4.84
DCC			4.23						
ECH1		-1.49	-1.20		-1.95	*			
ELF3	-1.27			2.06					
ELOVL3	-1.23	-1.46	-2.39						
ESRRA									-1.56
ESR2								1.31	2.44
ESRRG			-4.78			-2.59		1.66	
FASN		-1.84	-2.65			1.37	-2.23		
FGF2			3.52			6.18			
FOLH1	-1.34	-2.16		*	-2.56				
FOS	1.78			4.50				1.52	
FXRD5			-1.81			-1.87			
GAMT	-1.20								
GTF2H1	*	-1.42					-1.67		
HDAC6	*	-1.35					-1.63		
HGF	-1.95						-2.37	-2.03	-8.63
HMGB2		1.60	1.50		2.32	2.39			1.25
HSD17B2	1.78	2.12		1.78					-2.85
HSD3B1	-2.26	-2.95	-17.74		-2.41	-3.65	-3.61	-1.44	-4.01
IGF1	1.39	2.87							
IL18		-1.37							1.52
ISGF3G		-1.77	-1.88		-2.23	*	-2.00		
KISS1							-2.28		
LYPD3			-1.52			1.33		-2.05	-3.43
MMP2		-2.77	***					-1.75	-2.36
MMP9	-1.20								
MMP10	-1.48								
MORF4L2		-1.31	*					-1.47	-1.48
MTHFD2			2.83			2.40	*	-1.44	
MYC			2.27			5.18		-2.84	*
NCOA2		-1.32	-1.22						
NCOR1		-1.29	*					-1.48	
NFATC4		-1.95	-2.38		-2.78	*	-2.55	-1.37	-2.77
NOS3		1.20	2.12		-2.25	-2.25			1.44
NRG1	-2.26								
NR0B2		-2.40					-6.71		
NR4A3			1.32						1.26
OVGP1			1.20						
PECAM1	-2.00						-4.20	-1.45	-12.96
PLG	1.44		-1.79						
PPARGC1A	-2.59	-2.34	-57.73					-1.85	-9.35
PSCA	-1.47								-3.17
RERG	**	1.24			9.65				
RHOC	-1.21								
S100A4		-1.56	-2.35			1.47	-1.94	-1.27	-4.03
SERPINB5		-1.77	-2.59			1.25			-2.17
SERPINE1	-1.24	-1.29	-2.28			-2.82	-2.50	-1.90	
SET			1.33			1.40	-1.70		
SMAD2			1.30						
SMAD4			1.31						
SNCG		-1.42	-1.96		-1.86	-1.48		-2.32	-2.83
SPP1		-2.59	-6.74				-2.22	-1.76	-8.12
SSTR2			1.34			1.73	-1.95		
SULT2A1		-5.87	***						
SULT1E1	-7.91						-2.23		
TACSTD1			1.37						
TFF1		-2.21	-2.44		20.13	158.9			
TFRC			1.34			1.30			
TNFSF10			-2.14						
Twist1	-1.93	-2.32	-1.93		-1.97	-4.85			
UBC			1.34			1.29			
UGT1A3			-3.38			-2.00			
UGT2B15			-3.06			8.37			
VIP			-4.57			6.13			
WISP1	-1.93	-2.57	-2.25		-2.79	-2.13			
XDH		-4.02	-2.97			-1.21			-6.40
YWHAZ			1.41			1.78			

determined between 6 and 48 hours after the last treatment and a steady state of ~20 ng/mL was reached at 24 hours (Fig. 4A). The area under the curve ( $\mu\text{mol} \times \text{hours} / \text{L}$ ) was 3.5 and 4.1 for 15 and 30 mg/kg of compound A treatments, respectively. At 6 hours, the  $C_{\text{max}}$  was reached: 0.13  $\mu\text{mol}/\text{L}$  for the 15 mg/kg and 0.21  $\mu\text{mol}/\text{L}$  for the 30 mg/kg doses. The maximum achievable dose was determined to be 49.7 and 78.4 ng/mL (15 and 30 mg/kg, respectively) at 6 hours.

To determine if compound A would inhibit breast tumor growth, breast tumor xenografts were established in ovariectomized athymic nude mice. For the E2-dependent breast tumor model, MCF-7 cells were injected into the mammary fat pads of ovariectomized athymic nude mice implanted with an E2 pellet. After 5 weeks, tumor cross-sectional area reached 0.28  $\text{cm}^2$ , at which time, mice were treated with compound A or ICI-182,780 (Fig. 4B). After 2 weeks of treatment, a decrease in growth was observed in both treatment groups (Fig. 4B). Comparison of tumor size after 2, 3, and 4 weeks of treatment suggests that growth stabilization occurred in both the ICI-182,780 and compound A groups. The E2 control group tumors increased in size at a steady rate over time throughout the entire experiment reaching 0.6  $\text{cm}^2$ . At the final measurement, the compound A group tumor area was 0.3  $\text{cm}^2$  ( $P = 0.004$ ) whereas the ICI-182,780 tumor area was 0.2  $\text{cm}^2$  ( $P < 0.001$ ).

For the E2-independent breast tumor model, BT-20 tumors were similarly established in the axillary mammary fat pads of athymic nude mice. After 8 weeks, tumor cross-sectional area reached 0.2  $\text{cm}^2$  and the mice were treated with control vehicle or compound A (Fig. 4C). By the second week of treatment, inhibition of tumor growth by compound A was clearly seen. After 5 weeks of treatment, the vehicle group tumor size reached 0.5  $\text{cm}^2$ , whereas compound A treatment group tumor size was significantly smaller at 0.3  $\text{cm}^2$  ( $P = 0.007$ ). At the conclusion of the xenograft experiments, 4 days after the final treatment administration, the plasma concentration of compound A was determined to be 15.1 ng/mL in the MCF-7, and 17.9 ng/mL in the BT-20 xenograft model, consistent with the pharmacokinetic data (Fig. 4A).

#### Compound A Exhibits Antagonistic Effects on the Mouse Uterus

Uterine weight has been extensively used to monitor estrogen-mediated proliferative effects on the uterus (23). Therefore, at the end of the MCF-7 and BT-20 xenograft experiments, uterine weights were measured. As expected, the pure antiestrogen ICI-182,780 significantly decreased

**Figure 2.** Gene expression profiles of breast cancer cells treated with  $\text{ERR}\alpha$  antagonist compound A. MCF-7 and BT-20 cells were treated with 5  $\mu\text{mol}/\text{L}$  of compound A, 3  $\text{pmol}/\text{L}$  of E2, or vehicle control for 2, 24, and 72 h. Gene expression profiles were determined using low-density array card. Out of 226 genes assayed, 83 were down-regulated by  $\geq 1.2$ -fold or up-regulated by  $> 1.2$ -fold ( $P < 0.05$ ). *Green*, down-regulation; *red*, up-regulation. \*, a decrease in expression, but  $\leq 1.2$ ; \*\*, an increase in expression, but  $< 1.2$ . Values were included due to a trend seen in comparison to other time points. \*\*\*, expression was measured in vehicle sample, but upon treatment, amplification was not detectable. Comparison of relative gene expression (vehicle vs. treatment) was done using ANOVA followed by a Student's *t* test with a 0.05 significance level.

( $P < 0.001$ ) uterine weight in the MCF-7 xenograft study (Fig. 5A), whereas the ERR $\alpha$  antagonist compound A group also showed a slight decrease ( $P = 0.303$ ). Moreover, compound A significantly decreased ( $P = 0.013$ ) uterine weight in the BT-20 xenograft study (Fig. 5B). These data suggest that the ERR $\alpha$  antagonist compound A exhibits antagonistic effects on uterine growth.

To investigate the antagonistic effect caused by compound A in the uterus, 46 genes known to play a role in ERR $\alpha$  signaling (shown in bold in Fig. S1) were assayed using TaqMan Low-Density Custom Array cards. In this assay, we found that 18 genes were down-regulated  $\geq 1.2$  ( $P < 0.05$ ; Supplementary Fig. S2A).<sup>4</sup> Of these 18 genes down-regulated in the mouse uteri, 10 were also down-regulated in the MCF-7 and BT-20 cell lines treated with compound A (Fig. 2). Six genes (*ESRRG*, *FASN*, *LYPD3*, *MTHFD2*, *MYC*, and *SET*) that were up-regulated or down-regulated depending on the cell line and time point were all down-regulated in the mouse uteri. *CYP11B1* and *NR4A3* were up-regulated in both the MCF-7 and BT-20 cell lines but were both down-regulated in the mouse uteri. Importantly, 14 out of the 18 genes down-regulated in the mouse uteri by compound A were built into one signaling pathway involving ERR $\alpha$  (Supplementary Fig. S2B).<sup>4</sup> These data suggest that compound A also affects ERR $\alpha$  signaling in mouse uterus.

We have previously shown that compound A induces ERR $\alpha$  protein degradation in MCF-7 cells through the ubiquitin proteasome pathway,<sup>3</sup> and postulated that ERR $\alpha$  degradation leads to breast cancer cell growth inhibition. Thus, we established MCF-7/shERR $\alpha$  RNAi stable knock-downs<sup>3</sup> by transfecting MCF-7 cells with short hairpin RNA expression plasmids (SuperArray Bioscience Corporation) specific for ERR $\alpha$ . A short hairpin RNA expressing a scrambled artificial sequence that does not match any human, mouse, or rat gene was used as a negative control. Cell proliferation assays were done and the results show that knocking down ERR $\alpha$  led to the inhibition of breast cancer cell proliferation (Supplementary Fig. S3).<sup>4</sup> Additionally, knocking down ERR $\alpha$  led to the down-regulation of ACADM, CYP19A1, PGC-1 $\alpha$ , SPP1, and TFF1.<sup>3</sup> Likewise, ACADM, CYP19A1, PGC-1 $\alpha$ , SPP1, and TFF1 were down-regulated when MCF-7 cells were treated with compound A (Fig. 2).

## Discussion

This is the first demonstration that an ERR $\alpha$ -selective antagonist could inhibit the proliferation of breast cancer

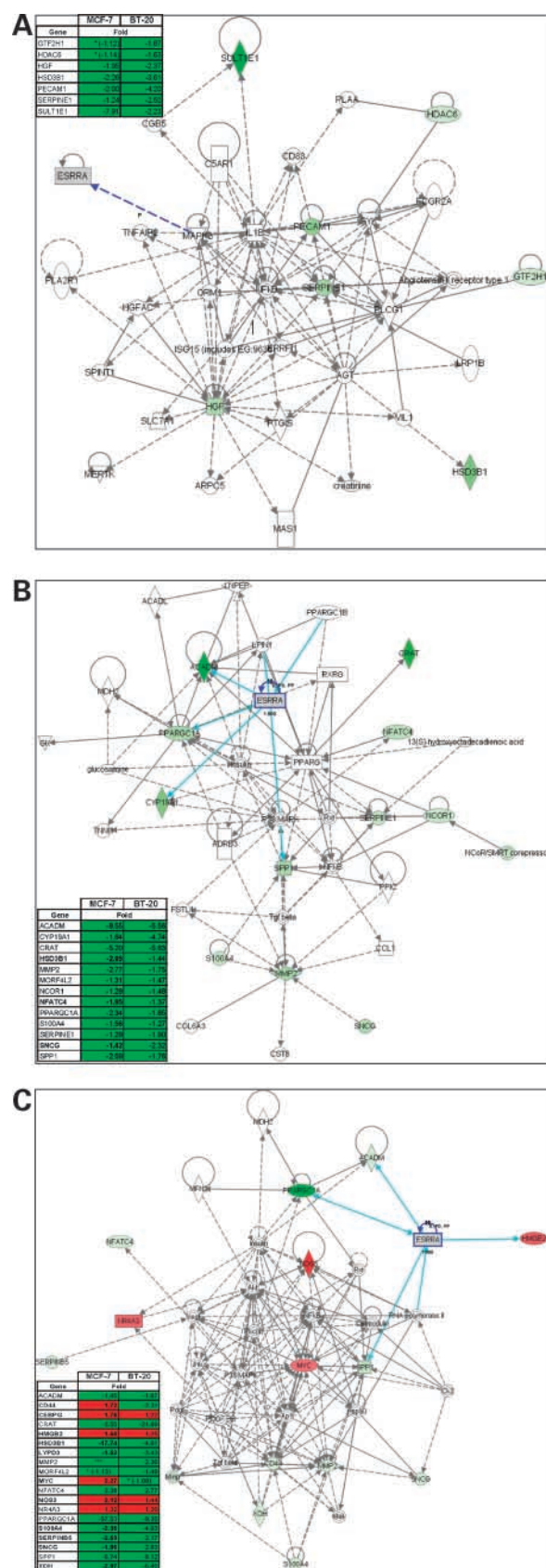


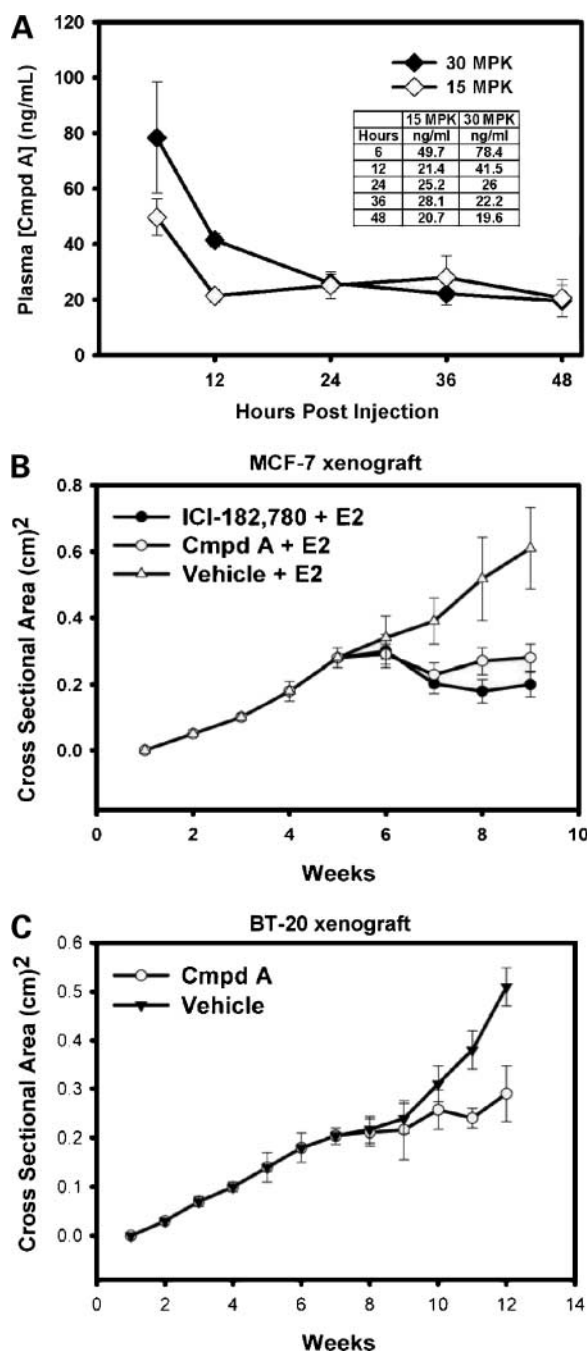
**Figure 3.** Signaling pathways affected by ERR $\alpha$  antagonist compound A in breast cancer cells. Relative gene fold expression data from MCF-7 and BT-20 cells treated with compound A for 2, 24, and 72 h were analyzed through the use of Ingenuity Pathway Analysis (Ingenuity Systems). Differentially expressed (vehicle vs. compound A) genes from both MCF-7 and BT-20 were analyzed at 2 h (A), 24 h (B), and 72 h (C). Genes in boldface (left) also responded to E2 treatment. Solid line, direct interaction (turquoise blue solid line, direct interaction with ERR $\alpha$ ); dotted line, indirect interaction. Green nodes, down-regulated; red nodes, up-regulated (for more information, see also <http://www.ingenuity.com/>).



678 *ERR $\alpha$  Antagonist Suppresses Breast Cancer Growth*

cells *in vitro* (Fig. 1) and slow tumor growth in mouse xenograft models (Fig. 4B and C). We have also investigated the molecular basis for this observation by examining changes in gene expression in breast cancer cell lines and tissue in response to the *ERR $\alpha$*  antagonist treatment (Figs. 2 and 3).

Is antagonizing *ERR $\alpha$*  leading to breast cancer cell and tumor inhibition mediated by the disruption of energy metabolism? We found that 11 genes that were down-regulated at 24 hours of treatment with compound A fit into a network involving energy metabolism (Fig. 3B).



Compound A down-regulates *ACADM*, which catalyzes the initial step in mitochondrial fatty acid oxidation. It has been well-established that *ERR $\alpha$*  is a direct regulator of *ACADM* (3, 24, 25). Likewise, the nuclear coactivator *PGC-1 $\alpha$*  was down-regulated. *PGC-1 $\alpha$*  is a key regulator of genes that control many important aspects of metabolism including glucose uptake, gluconeogenesis, mitochondrial biogenesis, and adaptive thermogenesis (26). *PGC-1 $\alpha$*  interacts with *ERR $\alpha$*  and potentiates transcriptional activity (4, 24, 27, 28). Moreover, a pathway describing coregulation of *ERR $\alpha$*  and *PGC-1 $\alpha$*  along with up-regulating *PPAR $\alpha$* , which in turn regulates *ACADM*, has also been described (29). Compound A treatment led to the down-regulation *LPIN1*, which is a *PGC-1 $\alpha$*  target gene, and is known to be involved in pathways that lead to the expression of genes involved in mitochondrial fatty acid oxidative metabolism.

Interestingly, *LPIN1* has also been shown to interact with *ERR $\alpha$*  (30). Also, other genes identified in this network involved in energy metabolism include malate dehydrogenase 2, which is found in the mitochondria where it plays a critical role in the malate-aspartate shuttle that catalyzes the oxidation of malate to oxaloacetate in the citric acid cycle (31). *ACADL* (long chain acyl-CoA dehydrogenase) takes part in catalyzing (along with *ACADM*) the initial step of mitochondrial fatty acid  $\beta$ -oxidation (32). Carnitine acetyltransferase catalyzes the transfer of acyl groups from acyl-CoA thioester to carnitine. It is a key enzyme for energy homeostasis and fat metabolism through the regulation of the ratio of acyl CoA/CoA in subcellular compartments (21). Therefore, given the key genes involved in energy metabolism that are disrupted upon treatment with compound A for 24 hours, it seems as though antagonizing *ERR $\alpha$*  in breast tumors can lead to tumor growth inhibition at least partly through affecting energy metabolism.

**Figure 4.** *ERR $\alpha$*  antagonist compound A inhibits breast tumor growth in mouse xenograft models. **A**, pharmacokinetic study of compound A in athymic nude mice. Ovariectomized, athymic nude mice implanted with an E2 pellet received 15 mg/kg of compound A, 30 mg/kg of compound A, or vehicle control for 5 consecutive days. Compound A plasma concentration was measured at 6, 12, 24, 36, and 48 h after day 5 article administration. **B**, compound A inhibits the growth of MCF-7 xenograft breast tumor. MCF-7 ( $1 \times 10^7$ ) cells/site were injected (s.c.) into the axillary mammary fat pads of ovariectomized, athymic nude mice that were also implanted with an E2 pellet. After 5 wk, mice were divided into three treatment groups: control vehicle, 15 mg/kg of compound A, and 5 mg/wk of ICI-182,780. Tumor cross-sectional area was determined weekly by Vernier calipers and calculated using the formula: length / 2  $\times$  width / 2  $\times$   $\pi$ . In comparison to the E2 control group, significant inhibition of growth was seen in both the ICI-182,780 and compound A groups. At week 9, the compound A group tumor area was 0.3 cm<sup>2</sup> (\*,  $P = 0.004$ ) whereas ICI-182,780 was 0.2 cm<sup>2</sup> (\*,  $P < 0.001$ ). **C**, compound A inhibits the growth of BT-20 xenograft breast tumor. BT-20 ( $5 \times 10^6$ ) cells/site were injected (s.c.) into the axillary mammary fat pads of athymic nude mice. After 8 wk, mice were divided into two treatment groups: control vehicle and 30 mg/kg Cmpd A. At week 12, the vehicle group tumor size had reached 0.5 cm<sup>2</sup> whereas compound A treatment group was significantly reduced by 0.3 cm<sup>2</sup> ( $P = 0.007$ ). Differences in mean tumor area between groups were measured by ANOVA followed by a Student's *t* test with a 0.05 significance level.

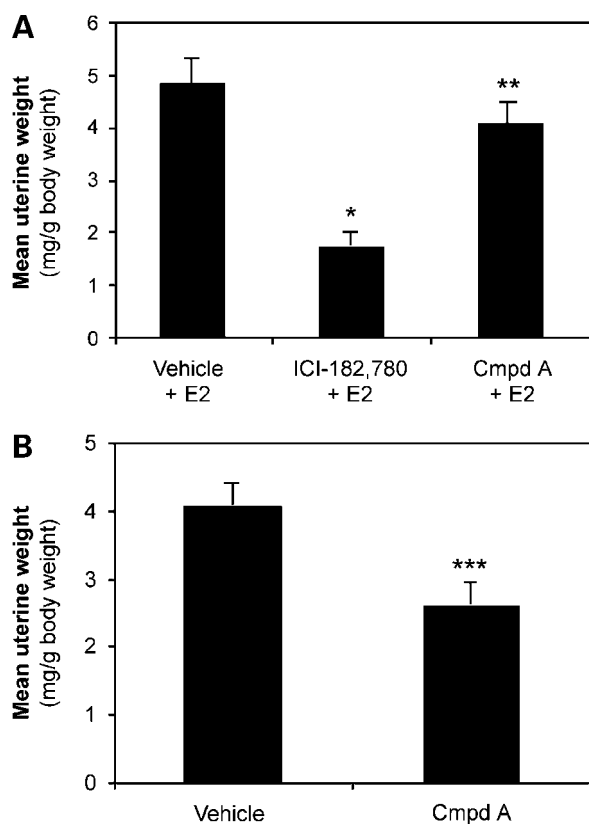


**Figure 5.** ERR $\alpha$  antagonist compound A reduces uterine weights of mice from breast cancer xenograft models. Whole body weights of mice were weighed; subsequently, uteri were excised, cleaned, and weighed from the same mice (from Fig. 4B and C) treated with (A) MCF-7 xenograft: vehicle, 5 mg/wk of ICI-182,780, or 15 mg/kg of compound A, or (B) BT-20 xenograft: vehicle or 30 mg/kg. \*,  $P < 0.001$ ; \*\*,  $P = 0.303$ ; and \*\*\*,  $P = 0.013$ . Differences in uteri/body weight between groups were measured by ANOVA followed by a Student's  $t$  test with a 0.05 significance level.

Along with the genes discussed above, compound A also down-regulated CYP19A1 and SPP1 in both MCF-7 and BT-20 cells treated for 24 hours (Figs. 2 and 3B). CYP19A1 (aromatase) is the estrogen synthetase that converts androgens to estrogens including E2, the potent natural ligand of ER. CYP19A1 is an ERR $\alpha$  target gene; it regulates the expression of aromatase (9). DES (at low concentrations that activate ER $\alpha$ ) and E2 treatment results in an increase of ERR $\alpha$  in the mouse uterus (33). Furthermore, ERR $\alpha$  increases aromatase expression in breast tissue (9), ERR $\alpha$  is a direct target of ER $\alpha$  activity, and ER $\alpha$  induces ERR $\alpha$  expression in the breast (33, 34). Moreover, ERR $\alpha$  stimulates the estrogen-responsive gene, *SPP1* (osteopontin; ref. 10). At 72 hours of treatment by compound A, 14 genes fit into a network involving ERR $\alpha$  signaling (Fig. 3C). In particular, the up-regulated HMGB2 is reported to have a broad architectural function in the assembly of nucleoprotein complexes involved in the regulation of transcription (22).

Additionally, it has been reported that ERR $\alpha$  increases the expression of HMGB2 in rat neonatal myocytes (29). Other interesting genes to note, the transcription factor

MYC, has been shown to bind the osteopontin promoter and promote up-regulation in astrocytic cells (35). Additionally, S100A4 (S100 calcium binding protein A4), shows elevated expression in cancer and contributes to tumor cell motility and metastatic progression (36). Moreover, S100A4 increases osteopontin (*SPP1*) expression (37) and SNCG. Therefore, antagonizing ERR $\alpha$  activity with compound A could result in the inhibition of ER $\alpha$  signaling and other estrogenic responses, which might also account for its inhibition of breast cancer cell lines and tumors.

It is of interest to point out that the networks built by Ingenuity Pathway Analysis (Fig. 3) did not include ER, which implies that these pathways are estrogen-independent. In the future, it will be interesting to compare gene expression data from multiple ER-negative breast cancer cell lines (MDA-MB-231, BT-20, and SKBR3) treated with an ERR $\alpha$  subtype-specific antagonist in order to identify key genes involved in ERR $\alpha$ -dependent/ER-independent signaling in breast cancer.

Due to the multiple interconnections between ER $\alpha$  and ERR $\alpha$ , we also looked at the effects of E2 treatment on genes known to be differentially expressed in breast cancer cells upon treatment with an ERR $\alpha$  subtype-specific antagonist yet were also estrogen responsive (Fig. 2). Although seven genes were differentially expressed in both MCF-7 and BT-20 breast cancer cells when treated for 2 hours with compound A, no effect was seen (on the same genes) after 2 hours of treatment with E2 (Figs. 2 and 3A). At 24 hours, although 11 genes were differentially expressed when treated with compound A and were built into one pathway; only 2 (*NFATC4* and *SNCG*) out of the 11 genes responded to E2 (Figs. 2 and 3B). *NFATC4* (nuclear factor of activated T-cells, cytoplasmic, calcineurin-dependent 4) is a transcriptional coactivator that regulates PPAR $\gamma$  and is involved in fat cell differentiation (38). Although PPAR $\gamma$  does not directly interact with ERR $\alpha$ , it interacts with LPIN1, ACADM, and PGC-1 $\alpha$  which all directly interact with ERR $\alpha$ . *SNCG* (synuclein- $\gamma$ ; breast cancer-specific protein 1) is not a well-understood protein that regulates matrix metalloproteinases, and is reported to be overexpressed in advanced infiltrating breast cancer. Furthermore, this overexpression increases invasion and metastasis in breast cancer. Additionally, although there have been no reports that *SNCG* interacts directly with ERR $\alpha$ , it has been reported that *SNCG* increases the activity of matrix metalloproteinase 2 (39). Moreover, it has been shown that osteopontin (*SPP1*) stimulates matrix metalloproteinase 2 activation (40). At 72 hours, 14 genes differentially expressed in breast cancer cells treated with compound A were modeled into a pathway involving ERR $\alpha$  signaling; 8 of the 14 genes modeled also responded to E2 (Figs. 2 and 3C). Of the eight genes that responded to compound A and E2 treatment, only one (*HMGB2*, described above) directly interacted with ERR $\alpha$ . Therefore, whereas an increase in genes that were both differentially expressed by compound A and E2 was observed over time, only one gene (*HMGB2*) directly interacted with ERR $\alpha$  when modeled by Ingenuity Pathway Analysis.



Given that ERR $\alpha$  can stimulate ER $\alpha$  target genes in the absence of estrogen, is it possible that ERR $\alpha$  stimulates and/or controls ER-independent cancer growth? Our BT-20 and MDA-MB-231 cell proliferation data (Fig. 1), along with our BT-20 xenograft results (Fig. 4), show that there are ERR $\alpha$  signaling pathways acting independent of ER $\alpha$ . By studying differential gene expression between the vehicle and compound A, we were able to focus on studying ERR $\alpha$  signaling that is independent of estrogen.

Additionally, growth inhibition by compound A in known ERR $\alpha$ -positive cells: CaCo-2 (colon), C2C12 (muscle), HEP G2 (liver), MG-63 (bone), RD (muscle), RL95-2 (uterus), and SAOS-2 (bone) were examined. Decreased proliferation of RL95-2 cells with compound A was exhibited (IC<sub>50</sub> = 250  $\mu$ mol/L), whereas no or little change on the other cell lines proliferation rates were affected by compound A (data not shown). Therefore, except at high concentrations in the endometrial RL95-2 cells, compound A exhibits a minimal affect on nonreproductive cells.

We have shown that compound A does not bind ER $\alpha$  in an ER $\alpha$ /coactivator homogenous time-resolved fluorescence assay (12). It is also known that ER $\alpha$  mRNA and protein are not significantly affected when MCF-7 cells are treated with compound A.<sup>3</sup> Yet interestingly, compound A acts as an antagonist in the uterus (Fig. 5). High levels of ERR $\alpha$  are known to be present in the uterus and it has been well-established that compounds exhibiting agonistic or antagonistic ER $\alpha$  activity can be monitored in the uterus (23). We have further analyzed the expression of 46 genes, which showed a robust effect in response to compound A treatment *in vitro*, in uteri from mice that were treated with ERR $\alpha$  antagonist. Eighteen genes were down-regulated in the mouse uteri, and 10 of them were also down-regulated in the MCF-7 and BT-20 cell lines treated with compound A (Supplementary Fig. S2).<sup>4</sup> These data suggest that compound A may affect ERR $\alpha$  signaling in the uterus. Furthermore, we have established that knocking-down ERR $\alpha$  in breast cancer cells led to inhibition of cell proliferation (Supplementary Fig. S3).<sup>4</sup> Future studies to further investigate these genes and the role of ERR $\alpha$  signaling in the uterus are of interest. Our data also imply an ERR $\alpha$ -dependent proliferative pathway that may be independent of ER $\alpha$ .

The ERR $\alpha$  knockout mouse is reported to have a reduced body weight, altered peripheral fat deposit and morphology, and show reduced lipogenesis (5). The knockout also exhibits significant fat malabsorption and steatorrhea (41). Interestingly, compound A did not significantly affect whole mouse body weights. In the MCF-7 xenograft model, the vehicle group weighed 22.5  $\pm$  1.5 g, the ICI-182,780 group weighed 24.3  $\pm$  0.61 g, and the compound A group weighed 24.5  $\pm$  0.43 g. Whereas in the BT-20 xenograft model, the vehicle group weighed 25.9  $\pm$  0.57 g and the compound A group weighed 25.2  $\pm$  0.44 g. Additionally, there was no observable toxicity seen in mice treated with compound A.

The success of targeting ER $\alpha$  to treat breast cancer with such drugs as tamoxifen and ICI-182,780 (faslodex) has

been well documented (42, 43). Future studies should include treating ER $\alpha$ -positive cells and mouse xenografts with combinations of tamoxifen, faslodex, or an aromatase inhibitor with compound A. Treating tamoxifen-resistant cells with compound A would also be of great interest. Although there are many successful therapies to breast cancer, tragically more than 40,000 women will still die this year. Consequently, there continues to be an unmet medical need for breast cancer treatments. Importantly, our *in vitro* and *in vivo* studies suggest that ERR $\alpha$  could be an effective target to treat breast cancer, independent of ER status.

## Disclosure of Potential Conflicts of Interest

M.J. Chisamore, H.A. Wilkinson, and O. Flores are employees of Merck Research Laboratories. No other potential conflicts of interest were disclosed.

## Acknowledgments

We thank Dr. Michael Gentile, Matt Borran, D.J. Ferraro, Ioan Petrescu, Kenneth Lodge, and James Destefano for help with *in vivo* studies. We also thank James Guare for providing medicinal chemistry support.

## References

- Giguere V, Yang N, Segui P, Evans RM. Identification of a new class of steroid hormone receptors. *Nature* 1988;331:91–4.
- Tremblay GB, Kunath T, Bergeron D, et al. Diethylstilbestrol regulates trophoblast stem cell differentiation as a ligand of orphan nuclear receptor ERR  $\beta$ . *Genes Dev* 2001;15:833–8.
- Sladek R, Bader JA, Giguere V. The orphan nuclear receptor estrogen-related receptor  $\alpha$  is a transcriptional regulator of the human medium-chain acyl coenzyme A dehydrogenase gene. *Mol Cell Biol* 1997;17:5400–9.
- Ichida M, Nemoto S, Finkel T. Identification of a specific molecular repressor of the peroxisome proliferator-activated receptor  $\gamma$  coactivator-1  $\alpha$  (PGC-1 $\alpha$ ). *J Biol Chem* 2002;277:50991–5.
- Luo J, Sladek R, Carrier J, Bader JA, Richard D, Giguere V. Reduced fat mass in mice lacking orphan nuclear receptor estrogen-related receptor  $\alpha$ . *Mol Cell Biol* 2003;23:7947–56.
- Lu D, Kiriya Y, Lee KY, Giguere V. Transcriptional regulation of the estrogen-inducible pS2 breast cancer marker gene by the ERR family of orphan nuclear receptors. *Cancer Res* 2001;61:6755–61.
- Yang N, Shigeta H, Shi H, Teng CT. Estrogen-related receptor, hERR1, modulates estrogen receptor-mediated response of human lactoferrin gene promoter. *J Biol Chem* 1996;271:5795–804.
- Zhang Z, Teng CT. Estrogen receptor-related receptor  $\alpha$ 1 interacts with coactivator and constitutively activates the estrogen response elements of the human lactoferrin gene. *J Biol Chem* 2000;275:20837–46.
- Yang C, Zhou D, Chen S. Modulation of aromatase expression in the breast tissue by ERR $\alpha$ -1 orphan receptor. *Cancer Res* 1998;58:5695–700.
- Vanacker JM, Delmarre C, Guo X, Laudet V. Activation of the osteopontin promoter by the orphan nuclear receptor estrogen receptor related  $\alpha$ . *Cell Growth Differ* 1998;9:1007–14.
- Xie W, Hong H, Yang NN, et al. Constitutive activation of transcription and binding of coactivator by estrogen-related receptors 1 and 2. *Mol Endocrinol* 1999;13:2151–62.
- Chisamore M, Mosley R, Cai S, et al. Identification of small molecule estrogen related receptor  $\alpha$  specific antagonists and homology modeling to predict the molecular determinants as the basis for selectivity over ERR $\beta$  and ERR $\gamma$ . *Drug Dev Res* 2008;69:203–18.
- Busch BB, Stevens WC, Jr., Martin R, et al. Identification of a selective inverse agonist for the orphan nuclear receptor estrogen-related receptor  $\alpha$ . *J Med Chem* 2004;47:5593–6.
- Kallen J, Lattmann R, Beerli R, et al. Crystal structure of human estrogen-related receptor  $\alpha$  in complex with a synthetic inverse agonist reveals its novel molecular mechanism. *J Biol Chem* 2007;282:23231–9.

15. Ariazi EA, Clark GM, Mertz JE. Estrogen-related receptor  $\alpha$  and estrogen-related receptor  $\gamma$  associate with unfavorable and favorable biomarkers, respectively, in human breast cancer. *Cancer Res* 2002;62:6510–8.
16. Suzuki T, Miki Y, Moriya T, et al. Estrogen-related receptor  $\alpha$  in human breast carcinoma as a potent prognostic factor. *Cancer Res* 2004;64:4670–6.
17. Marselos M, Tomatis L. Diethylstilboestrol: I. Pharmacology, toxicology and carcinogenicity in humans. *Eur J Cancer* 1992;28A:1182–9.
18. Horwitz KB, Zava DT, Thilagar AK, Jensen EM, McGuire WL. Steroid receptor analyses of nine human breast cancer cell lines. *Cancer Res* 1978;38:2434–7.
19. Najid A, Habrioux G. Biological effects of adrenal androgens on MCF-7 and BT-20 human breast cancer cells. *Oncology* 1990;47:269–74.
20. Taylor CM, Blanchard B, Zava DT. Estrogen receptor-mediated and cytotoxic effects of the antiestrogens tamoxifen and 4-hydroxytamoxifen. *Cancer Res* 1984;44:1409–14.
21. van der Leij FR, Huijman NC, Boomsma C, Kuipers JR, Bartelds B. Genomics of the human carnitine acyltransferase genes. *Mol Genet Metab* 2000;71:139–53.
22. Melvin VS, Harrell C, Adelman JS, Kraus WL, Churchill M, Edwards DP. The role of the C-terminal extension (CTE) of the estrogen receptor  $\alpha$  and  $\beta$  DNA binding domain in DNA binding and interaction with HMGB. *J Biol Chem* 2004;279:14763–71.
23. Owens JW, Ashby J. Critical review and evaluation of the uterotrophic bioassay for the identification of possible estrogen agonists and antagonists: in support of the validation of the OECD uterotrophic protocols for the laboratory rodent. Organisation for Economic Co-operation and Development. *Crit Rev Toxicol* 2002;32:445–520.
24. Huss JM, Kopp RP, Kelly DP. Peroxisome proliferator-activated receptor coactivator-1 $\alpha$  (PGC-1 $\alpha$ ) coactivates the cardiac-enriched nuclear receptors estrogen-related receptor- $\alpha$  and - $\gamma$ . Identification of novel leucine-rich interaction motif within PGC-1 $\alpha$ . *J Biol Chem* 2002;277:40265–74.
25. Vega RB, Kelly DP. A role for estrogen-related receptor  $\alpha$  in the control of mitochondrial fatty acid  $\beta$ -oxidation during brown adipocyte differentiation. *J Biol Chem* 1997;272:31693–9.
26. Puigserver P, Spiegelman BM. Peroxisome proliferator-activated receptor- $\gamma$  coactivator 1 $\alpha$  (PGC-1 $\alpha$ ): transcriptional coactivator and metabolic regulator. *Endocr Rev* 2003;24:78–90.
27. Laganier J, Tremblay GB, Dufour CR, Giroux S, Rousseau F, Giguere V. A polymorphic autoregulatory hormone response element in the human estrogen-related receptor  $\alpha$  (ERR $\alpha$ ) promoter dictates peroxisome proliferator-activated receptor  $\gamma$  coactivator-1 $\alpha$  control of ERR $\alpha$  expression. *J Biol Chem* 2004;279:18504–10.
28. Schreiber SN, Knutti D, Brogli K, Uhlmann T, Kralli A. The transcriptional coactivator PGC-1 regulates the expression and activity of the orphan nuclear receptor estrogen-related receptor  $\alpha$  (ERR $\alpha$ ). *J Biol Chem* 2003;278:9013–8.
29. Huss JM, Torra IP, Staels B, Giguere V, Kelly DP. Estrogen-related receptor  $\alpha$  directs peroxisome proliferator-activated receptor  $\alpha$  signaling in the transcriptional control of energy metabolism in cardiac and skeletal muscle. *Mol Cell Biol* 2004;24:9079–91.
30. Finck BN, Gropler MC, Chen Z, et al. Lipin 1 is an inducible amplifier of the hepatic PGC-1 $\alpha$ /PPAR $\alpha$  regulatory pathway. *Cell Metab* 2006;4:199–210.
31. Burgess SC, Leone TC, Wende AR, et al. Diminished hepatic gluconeogenesis via defects in tricarboxylic acid cycle flux in peroxisome proliferator-activated receptor  $\gamma$  coactivator-1 $\alpha$  (PGC-1 $\alpha$ )-deficient mice. *J Biol Chem* 2006;281:19000–8.
32. Vega RB, Huss JM, Kelly DP. The coactivator PGC-1 cooperates with peroxisome proliferator-activated receptor  $\alpha$  in transcriptional control of nuclear genes encoding mitochondrial fatty acid oxidation enzymes. *Mol Cell Biol* 2000;20:1868–76.
33. Shigeta H, Zuo W, Yang N, DiAugustine R, Teng CT. The mouse estrogen receptor-related orphan receptor  $\alpha$ 1: molecular cloning and estrogen responsiveness. *J Mol Endocrinol* 1997;19:299–309.
34. Liu D, Zhang Z, Gladwell W, Teng CT. Estrogen stimulates estrogen-related receptor  $\alpha$  gene expression through conserved hormone response elements. *Endocrinology* 2003;144:4894–904.
35. Wang D, Yamamoto S, Hijiya N, Benveniste EN, Gladson CL. Transcriptional regulation of the human osteopontin promoter: functional analysis and DNA-protein interactions. *Oncogene* 2000;19:5801–9.
36. Tarabykina S, Griffiths TR, Tulchinsky E, Mellon JK, Bronstein IB, Kriajevska M. Metastasis-associated protein S100A4: spotlight on its role in cell migration. *Curr Cancer Drug Targets* 2007;7:217–28.
37. Duarte WR, Shibata T, Takenaga K, et al. S100A4: a novel negative regulator of mineralization and osteoblast differentiation. *J Bone Miner Res* 2003;18:493–501.
38. Yang TT, Xiong Q, Enslin H, Davis RJ, Chow CW. Phosphorylation of NFATc4 by p38 mitogen-activated protein kinases. *Mol Cell Biol* 2002;22:3892–904.
39. Surgucheva IG, Sivak JM, Fini ME, Palazzo RE, Surguchov AP. Effect of  $\gamma$ -synuclein overexpression on matrix metalloproteinases in retinoblastoma Y79 cells. *Arch Biochem Biophys* 2003;410:167–76.
40. Philip S, Bulbule A, Kundu GC. Osteopontin stimulates tumor growth and activation of promatrix metalloproteinase-2 through nuclear factor- $\kappa$ B-mediated induction of membrane type 1 matrix metalloproteinase in murine melanoma cells. *J Biol Chem* 2001;276:44926–35.
41. Carrier JC, Deblois G, Champigny C, Levy E, Giguere V. Estrogen-related receptor  $\alpha$  (ERR $\alpha$ ) is a transcriptional regulator of apolipoprotein A-IV and controls lipid handling in the intestine. *J Biol Chem* 2004;279:52052–8.
42. Howell A, Robertson JF, Quaresma Albano J, et al. Fulvestrant, formerly ICI 182,780, is as effective as anastrozole in postmenopausal women with advanced breast cancer progressing after prior endocrine treatment. *J Clin Oncol* 2002;20:3396–403.
43. Jordan VC, O'Malley BW. Selective estrogen-receptor modulators and antihormonal resistance in breast cancer. *J Clin Oncol* 2007;25:5815–24.

# Molecular Cancer Therapeutics

## Estrogen-related receptor- $\alpha$ antagonist inhibits both estrogen receptor-positive and estrogen receptor-negative breast tumor growth in mouse xenografts

Michael J. Chisamore, Hilary A. Wilkinson, Osvaldo Flores, et al.

*Mol Cancer Ther* 2009;8:672-681. Published OnlineFirst March 10, 2009.

<b>Updated version</b>	Access the most recent version of this article at: doi: <a href="https://doi.org/10.1158/1535-7163.MCT-08-1028">10.1158/1535-7163.MCT-08-1028</a>
<b>Supplementary Material</b>	Access the most recent supplemental material at: <a href="http://mct.aacrjournals.org/content/suppl/2009/03/04/1535-7163.MCT-08-1028.DC1">http://mct.aacrjournals.org/content/suppl/2009/03/04/1535-7163.MCT-08-1028.DC1</a>

<b>Cited articles</b>	This article cites 43 articles, 28 of which you can access for free at: <a href="http://mct.aacrjournals.org/content/8/3/672.full#ref-list-1">http://mct.aacrjournals.org/content/8/3/672.full#ref-list-1</a>
<b>Citing articles</b>	This article has been cited by 12 HighWire-hosted articles. Access the articles at: <a href="http://mct.aacrjournals.org/content/8/3/672.full#related-urls">http://mct.aacrjournals.org/content/8/3/672.full#related-urls</a>

<b>E-mail alerts</b>	<a href="#">Sign up to receive free email-alerts</a> related to this article or journal.
<b>Reprints and Subscriptions</b>	To order reprints of this article or to subscribe to the journal, contact the AACR Publications Department at <a href="mailto:pubs@aacr.org">pubs@aacr.org</a> .
<b>Permissions</b>	To request permission to re-use all or part of this article, use this link <a href="http://mct.aacrjournals.org/content/8/3/672">http://mct.aacrjournals.org/content/8/3/672</a> . Click on "Request Permissions" which will take you to the Copyright Clearance Center's (CCC) Rightslink site.